Journal of Pathology
J Pathol March 2021; **253:** 304–314
Published online 22 January 2021 in Wiley Online Library (wileyonlinelibrary.com) DOI: 10.1002/path.5588

ORIGINAL PAPER

Basal microvilli define the metabolic capacity and lethal phenotype of pancreatic cancer

Xu Han[1†], Lixiang Ma[2†], Jichun Gu[3†], Dansong Wang[1], Ji Li[3*], Wenhui Lou[1*], Hexige Saiyin[4*] and Deliang Fu[3]

[1] *Department of General Surgery, Zhongshan Hospital, Fudan University, Shanghai, PR China*
[2] *Department of Anatomy, Histology & Embryology, School of Medical Sciences, Fudan University, Shanghai, PR China*
[3] *Department of Pancreatic Surgery, Pancreatic Disease Institute, Huashan Hospital, Fudan University, Shanghai, PR China*
[4] *State Key Laboratory of Genetic Engineering, School of Life Sciences, Fudan University, Shanghai, PR China*

**Correspondence to: H Saiyin, State Key Laboratory of Genetic Engineering, School of Life Sciences, Fudan University, C223, Life Science Building, 2005 Songhu Road, Shanghai 200438, PR China. E-mail: saiyin@fudan.edu.cn; or W Lou, Department of General Surgery, Zhongshan Hospital, Fudan University, 130 Yixueyuan Road, Shanghai 20032, PR China. E-mail: lou.wenhui@zs-hospital.sh.cn; or J Li, Department of Pancreatic Surgery, Huashan Hospital, Fudan University, 12 Middle Wulumuqi Road, Shanghai 200040, PR China. E-mail: liji@huashan.org.cn*

[†]These authors contributed equally to this study.

Abstract

Apical microvilli of polarized epithelial cells govern the absorption of metabolites and the transport of fluid in tissues. Previously, we reported that tall and dense basal microvilli present on the endothelial cells of pancreatic cancers, a lethal malignancy with a high metabolism and unusual hypomicrovascularity, contain nutrient trafficking vesicles and glucose; their length and density were related to the glucose uptake of pancreatic cancers in a small-scale analysis. However, the implications of basal microvilli on pancreatic cancers are unknown. Here, we evaluated the clinical implications of basal microvilli in 106 pancreatic cancers. We found that basal microvilli are a dominant change in pancreatic cancers. The presence of longer and denser basal microvilli on the microvessels in pancreatic cancer tissues positively correlated with increased glucose uptake and higher metastatic (or invasive) and proliferative potentials of neoplastic cells and vice versa. Clinically, postoperative patients with longer and denser basal microvilli were more prone to unfavorable pathological characteristics and dismal prognoses. They were even more refractory to adjuvant therapy than those with shorter and thinner basal microvilli were. Our findings show that basal microvilli define the metabolic capacity and lethal phenotype of pancreatic cancers.

Keywords: basal microvilli; pancreatic cancer; glucose uptake; lethal phenotype; microvessel

Received 7 September 2020; Revised 22 October 2020; Accepted 2 November 2020

No conflicts of interest were declared.

Introduction

Apical microvilli of the polarized epithelia govern the absorptive and transporting capacity of metabolites and fluid in human tissues. Abundant apical microvilli are present in the epithelial cells of the small intestine and renal proximal tubule, where massive exchanges of metabolites and fluid occur [1–4]. Pancreatic cancer is a highly metabolic and almost incurable tumor with unusual hypomicrovascularity and dense stroma [5–7]. Dense desmoplastic stroma and hypomicrovascularity in the pancreatic cancer milieu block the delivery of therapeutic agents to the tumor and lead to a grim outcome for the patient [8,9]. However, nutrients, including glucose, glutamine, and albumin, quickly reach the tumor milieu and efficiently support tumor growth and metabolism [8,10]. Previously, we described a recently recognized anatomical structure, basal microvilli, which are preferentially present on the basal surface of polarized endothelial cells in pancreatic cancer tissues; they traverse dense stroma and are close to neoplastic cells [11]. Basal microvilli contain pinocytic and macropinocytic vesicles and glucose and do not depend on angiogenesis [11,12]. Principally, densely packed and long microvilli infer the high exchanging capacity of epithelial tissue [1,13]. Thus, the dynamics of basal microvilli might define the glucose metabolic capacity and lethal phenotype of pancreatic cancers.

Apical microvilli increase the surface area and enrich membrane-associated molecules for absorbing nutrients [2]. Apical microvilli on epithelial tissues are highly efficient in selectively exchanging nutrients and waste. Atrophy of the intestinal microvilli causes life-threatening watery diarrhea in microvillus inclusion disease [14,15]. Microvilli of syncytiotrophoblast cells in

the placenta also facilitate bidirectional feto-maternal exchanges [13]. We found that macropinocytic, pinocytic, Glut1-positive vesicles, and glucose appear in the lumen of basal microvilli [11,12]. Therefore, basal microvilli might compensate for the hypomicrovascularity in pancreatic cancer tissues and selectively deliver nutrients such as glucose to the tumor milieu rather than drugs such as nucleoside analogs. By analyzing seven patient samples, we found that longer and denser basal microvilli are related to higher glucose uptake in pancreatic cancer [11]. Higher glucose uptake in pancreatic cancer indicates a poor prognosis after surgery [16–19]. Therefore, the dynamics of basal microvilli might reflect the strengthening of glucose metabolic capacity, metastasis, aggressiveness, and chemoresistance of neoplastic cells in pancreatic cancers and predict the patient's outcome.

This study analyzed the basal microvilli parameters in 106 consecutive pancreatic cancer patients and the implications of basal microvilli in disease progression after surgery. We aimed to determine the implications of basal microvilli on the biology of neoplastic cells, including nutrient uptake, proliferation, and metastatic (or invasive) potential, and to define the relationships between the basal microvilli parameters and the clinicopathological characteristics of pancreatic cancer patients and the clinical values of basal microvilli for predicting postoperative chemoresistance and prognosis.

Patients and methods

Patient selection, data collection, and ethics

This prospective study enrolled 106 consecutive pancreatic cancer patients who underwent radical surgical resection in two medical centers from May 2013 to December 2018. Patients were excluded if neoadjuvant chemotherapy had been administered preoperatively. The ethics committee of Huashan/Zhongshan Hospital of Fudan University approved the study and informed consent was obtained from each patient. We have included the seven patients in our previous publication [11]. The basal microvilli parameters in tumor tissues were measured postoperatively, alongside postoperative pathological assessments. Standard demographic and clinicopathological data were obtained from the Pancreatic Tumor Registry and analyzed simultaneously. The basal microvilli parameters included their length and density, which were used to test the correlations of basal microvilli with clinicopathological features and prognosis. After the operation, patients were referred to the department of oncology for adjuvant therapy.

Immunofluorescence staining and antibodies

Details of the antibodies and software used are provided in supplementary material, Table S1.

Tissue collection and staining were conducted according to a method described previously [11]. In brief, thin slices of tumor samples were obtained and put into fresh 4% paraformaldehyde (PFA) for fixation. The tissue was dehydrated in 30% sucrose, frozen, and cryosectioned (45 μm). Sections were incubated in a blocking buffer and then incubated in a primary antibody solution overnight at 4 °C. Next, the sample was incubated for 1 h in the appropriate secondary antibody solution containing DAPI [donkey anti-rabbit Alexa 488 (Cat # A32790, 1/1000 dilution; Thermo Fisher, Rockford, IL, USA) or donkey anti-mouse Alexa 555 or Cy3 (Cat # A-31570, 1/1000 dilution; Thermo Fisher; or Cat # 715-167-003, 1/1000 dilution; Jackson Lab, Philadelphia, PA, USA)]. Finally, the immunostained sections were mounted on slides. Zeiss 710 or 880 confocal microscopy (ZEISS, Jena, Germany) with Z-stack and tile scanned images was performed. CD34 antibody (Cat # ab8536, 1/1000 dilution; Abcam, Cambridge, MA, USA) and cytokeratin-19 (CK-19) antibody (Cat # ab52625, 1/500 dilution; Abcam) or GLUT-1 antibody (Cat # ab115730, 1/200 dilution; Abcam) were used to stain the microvessels and neoplastic cells, respectively.

PET-CT scanning

The scanning settings for the VCT 64 PET/CT scanner (GE Medical Systems, Waukesha, WI, USA) were 140 kV and 200 mA. Each patient was injected with 0.1 mCi/kg body weight of ^{18}F-FDG as a tracer. Three-dimensional whole-body PET acquisitions were performed at three time points with nominal start times at 40, 65, and 90 min after the injection. The filtered back-projection (FBP) method was applied for image reconstruction. The maximum standardized uptake value (SUVmax) was quantified on the PET/CT images by two experienced nuclear radiologists.

Measurements of the basal microvilli parameters

ImageJ software (Fiji, NIH, Bethesda, MD, USA) was used to measure and analyze basal microvilli parameters as previously described [8]. We quantified the basal microvilli's length and density on the microvessels of pancreatic cancer in a 4- to 15-image Z-stack taken using a 63× objective. The mean/median values of length and density were considered as the basal microvilli parameters of patients (supplementary material, Table S2). The basal microvilli index was calculated as $[\pi \times 1 \times \text{length} \times \text{density}]/100$. Imaris 9.5 (Bitplane AG, Zürich, Switzerland) was used to visualize the surface.

Patient follow-up

MRI/CT or PET-CT scanning, serum CA 19-9, clinical symptoms, and physical examinations were documented for postoperative surveillance. Follow-up information was collected from the Pancreatic Tumor Registry, Fudan University. Radiological examinations were performed every 6 months or any time the patients had symptoms related to signs of recurrence. Recurrence was defined as radiological evidence of intra-abdominal soft tissue around the surgical site or distant metastasis with or without CA 19-9 > 37 U/ml during postoperative surveillance. The duration of overall survival (OS) was calculated from

Table 1. Clinicopathological characteristics of the pancreatic cancer patients.

			RFS univariate		OS univariate	
Clinical variables		**Count (%)**	*p*	**HR 95% CI**	*p*	**HR 95% CI**
Gender	Female	44 (41.5)	0.54	1.140 (0.748–1.738)	0.785	0.928 (0.541–1.592)
	Male	62 (58.5)				
Age	<60	30 (28.3)	0.33	0.799 (0.507–1.259)	0.718	0.899 (0.502–1.1.607)
	≥60	76 (71.7)				
Tumor stage	T1 + T2	73 (68.9)	0.26	1.286 (0.828–1.998)	**0.028**	**1.857 (1.069–3.228)**
	T3 + T4	33 (31.1)				
RLM	Yes	67 (36.8)	**0.00**	**2.217 (1.408–3.490)**	**0.008**	**2.261 (1.235–4.141)**
	No	39 (63.2)				
TNM	I + II	89 (84.0)	0.14	1.512 (0.878–2.606)	**0.007**	**1.420 (1.103–1.830)**
	III + IV	17 (16.0)				
PNI	Yes	74 (69.8)	0.81	1.0517 (0.668–1.672)	0.48	0.821 (0.475–1.419)
	No	32 (30.2)				
MVI	Yes	37 (34.9)	0.51	1.158 (0.746–1.798)	**0.013**	**1.964 (1.150–3.355)**
	No	69 (65.1)				
Tumor vascular thrombus	Yes	27 (25.5)	**0.00**	**2.084 (1.279–3.396)**	**0.002**	**2.720 (1.463–5.056)**
	No	79 (74.5)				
Resectional margin	R1	17 (16.0)	**0.03**	**1.824 (1.057–3.146)**	**0.133**	**1.660 (0.857–3.217)**
	R0	89 (84.0)				
CA 19-9	Positive	92 (86.8)	0.91	1.036 (0.561–1.915)	0.715	1.151 (0.540–2.452)
	Negative	14 (13.2)				
CEA	Positive	31 (29.2)	0.92	1.023 (0.648–1.615)	0.818	1.072 (0.592–1.940)
	Negative	75 (70.8)				
Ki67 index	<30%	46 (43.8)	0.55	1.134 (0.748–1.719)	0.194	1.430 (0.837–2.446)
	≥30%	59 (56.2)				
PET-CT	<6.5	34 (32.1)				
	>6.5	40 (37.7)	<0.001	3.312 (1.971–5.565)	**<0.001**	**3.565 (1.809–7.024)**
	NA	32 (30.1)				
Adjuvant therapy	Chemo	87 (82.1)				
	Chemo + radio	10 (9.4)	0.33	0.675 (0.308–1.476)	0.45	1.427 (0.567–3.593)
	No	9 (8.5)				
Relapse	Yes	91 (85.8)	Median DFS: 298 ± 28			
	No	15 (14.2)				
Survival	Alive	49 (46.2)	Median OS: 585 ± 43			
	Died	57 (53.8)				

MVI, major vascular invasion; PNI, perineural invasion; RLM, regional lymph metastasis.
Bold font indicates statistically significant values.

the date of surgery to the date of tumor-specific death or the last follow-up visit date. Relapse-free survival (RFS) was calculated as the time from surgery to the time of recurrence.

Chemotherapy and chemoradiotherapy

Patients received gemcitabine (1000 mg/m^2 over 30 min) on days 1, 8, and 15 of a 28-day cycle, or gemcitabine (1000 mg/m^2 over 30 min) on days 1 and 8 with concurrent S-1 (40–60 mg/m^2) orally twice daily on days 1–14 of a 21-day cycle. The adjuvant chemoradiotherapy dose was 50.4 Gy in 25–28 fractions and was given concurrently with S-1 (40 mg) orally twice daily during the radiation day.

Statistical analyses

The statistical analyses were performed using SPSS version 21.0 (SPSS Inc, Chicago, IL, USA) and R version 3.3.0 (http://www.r-project.org/). Pearson or Spearman correlation analysis was also performed to compare the correlations. Receiver operating characteristic (ROC) curves were used to evaluate the prognosis prediction of basal microvilli parameters. Survival curves were estimated according to the Kaplan–Meier method and were compared using the log-rank test. A Cox proportional hazards model was utilized for univariate analysis.

Results

General data

One hundred and six consecutive patients from two pancreatic cancer centers were recruited in this study (Table 1). Sixty-two samples (58.5%) were collected from the Department of Pancreatic Surgery, Zhongshan Hospital between May 2013 and December 2018; 44 (41.5%) were collected from the Pancreatic Cancer Center of Huashan Hospital between December 2016 and December 2018. The longest duration of follow-up was 1187 days, and the shortest was 133 days. The median follow-up time was 419 days. The median RFS time was 298 ± 28 days (± SEM), and the median OS was 585 ± 43 days (± SEM). Ninety-one patients (85.9%) relapsed after radical surgery, and 57 patients (53.8%) died during the follow-up period (Table 1). Resection margins, including transection and

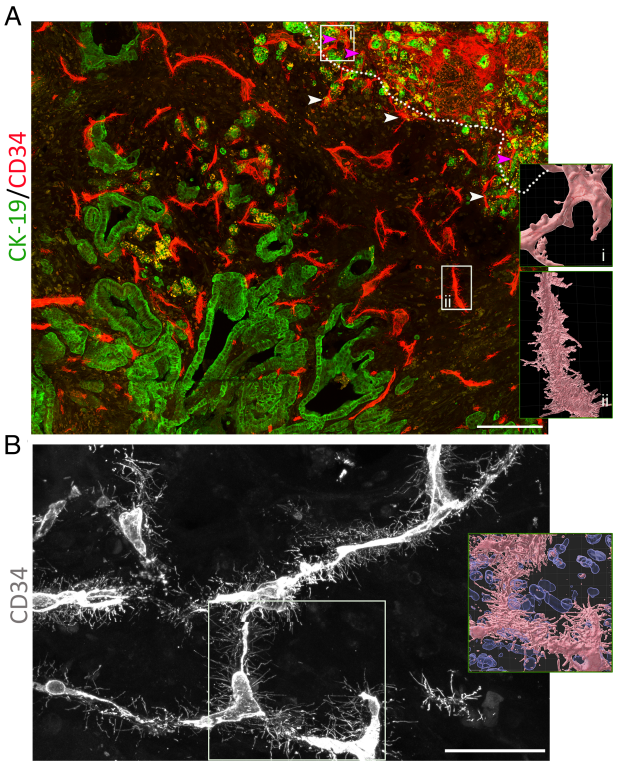

Figure 1. Basal microvilli are distinct characteristics of the microvasculature in pancreatic cancer. (A) Almost all microvessels in the pancreatic cancer region present basal microvilli but not those in the non-tumor region. (White dotted line indicates the margin of a tumor; white arrowheads indicate typical microvessels with basal microvilli; and pink arrowheads the microvessels in non-tumor pancreatic tissue.) Microvessels were stained for CD34 (red), and neoplastic cells for CK19 (green). Scale bar: 200 μm. (B) The patterns of basal microvilli present on the smaller branches of the microvessel network in pancreatic cancer. Scale bar: 50 μm. Microvessels were stained for CD34 (gray). For A and B, the right-hand-side panels show the surface of basal microvilli on microvessels (pink) and, where shown, cell nuclei (blue). Tile scanning with a Z-stack using a 63× objective; the images were stitched and shown as maximum intensity projection. The total area includes 48 fields in A and six fields in B. Images were processed using Imaris 9.6 software to visualize the microvasculature surface.

circumferential margins, were classified as R0 (distance from the margin to the tumor ≥ 1 mm) or R1 (distance from the margin to the tumor < 1 mm). Ninety-seven patients (91.5%) received chemotherapy-based treatment after surgery, including gemcitabine with or without concurrent S-1 or radiotherapy, and nine patients (8.5%) did not receive any adjuvant treatment (Table 1).

Basal microvilli are distinct characteristics of the microvasculature in pancreatic cancer

Basal microvilli are tiny, hair-like endothelial projections on the surface of the basal side of endothelia and can be visualized by high-resolution 3D confocal scans [11]. We have reported the patterns of basal microvilli on the microvessel segments in pancreatic cancers [11]. The depth and width of basal microvilli on the entire microvasculature nets in pancreatic cancer have not been reported. To see the basal microvilli patterns on the entire microvasculature nets of pancreatic cancer tissues, we visualized the whole networks of basal microvilli microvessels throughout the tumor region's non-cancerous tissue by an extensive area stitching technique after CD34 and CK-19 antibody immunostaining in 45-μm-thick sections. We observed that the basal microvilli were distinct features and systemic changes in the pancreatic cancer microvasculature system (Figure 1A), and were mostly enriched in the smaller branches of the microvasculature networks (Figure 1B). Consistent with our previous studies [8], basal microvilli also existed on the microvasculature of the invasive frontier of the tumor (Figure 1A). Surprisingly, the microvessel networks in pancreatic islets that were surrounded by neoplastic cells did not present basal microvilli, but the surrounding microvessels in the tumor region presented with long and dense basal microvilli (supplementary material, Figure S1A). We also observed that extremely long, thick, and dense basal microvilli presented on the primary pancreatic cancer tissue microvasculature with distant metastasis to the liver (supplementary material, Figure S1B). These findings further indicated that basal microvilli were tumor-specific and indicated the metabolic capacity of tumors rather than healthy pancreatic tissues, reflecting the metastatic and invasive potential of neoplastic cells in pancreatic cancers.

Longer and denser basal microvilli are related to the increased glucose uptake, higher metastatic or invasive and proliferative potential of neoplastic cells in pancreatic cancer

To analyze these basal microvilli on the microvasculature in pancreatic cancers, we used immunofluorescence for CD34 and glucose transporter-1 (GLUT-1) or cytokeratin-19 (CK-19) on five to ten cryosections cut at 45 μm thickness. After staining, we scanned the slices using a 63× objective to find microvessels with basal microvilli, and compared the length and density of the basal microvilli on different microvessels. After finding the microvessels with longer and denser basal microvilli compared with other microvessels, we scanned 4–15 images from each patientVs tumor tissue, used 3D reconstruction, and then measured the length and density of the basal microvilli. Among 106 patients, imaging showed that the microvasculature presented basal microvilli in 103 patients, and that the microvasculature in three patients did not present basal microvilli. We previously reported that an abundance of basal microvilli was closely correlated with increased PET-SUVmax values in seven patients [11]. In this cohort, 74 patients had PET-CT scanning before surgery. Our correlation analysis showed that longer and denser basal microvilli significantly correlated with a higher PET-SUVmax value (Figure 2A). The higher the PET-CT SUVmax value of the tumor tissue, the longer and denser were the basal microvilli that presented in the microvasculature of the same region (Figure 2A). Moreover, we observed that a 'flourishing' basal microvilli pattern with widespread branches from the microvasculature in pancreatic cancer tissues reflected extremely high PET-CT SUVmax

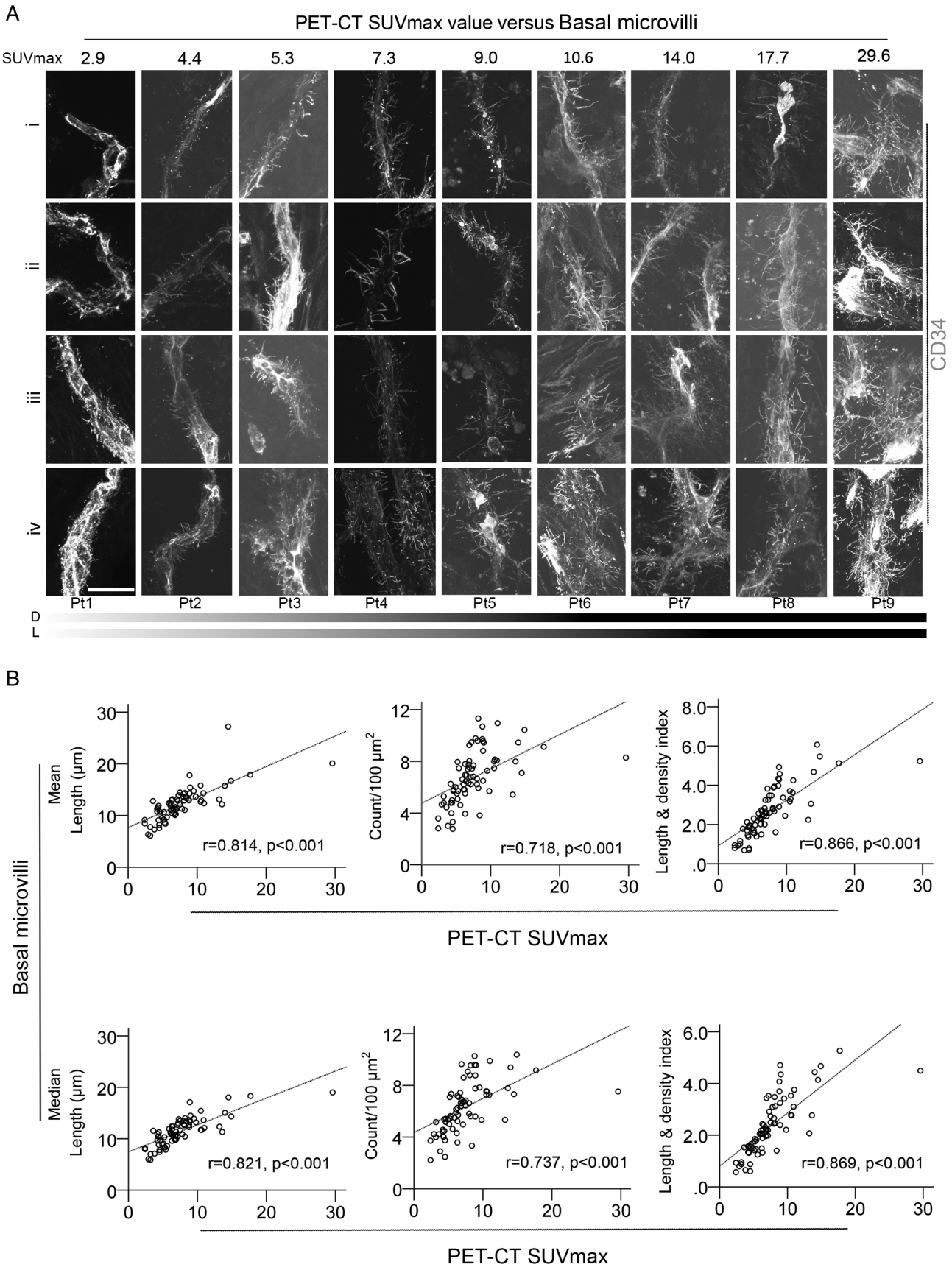

Figure 2. Longer and denser basal microvilli in pancreatic cancer indicate an elevated glucose uptake. (A) Typical patterns of basal microvilli on the microvasculature segments of nine pancreatic cancers with differential PET-CT SUVmax values. A CD34 antibody was used to stain microvessels. All images were taken from a Z-stack and are shown as maximum intensity projection. Scale bar: 20 μm. (B) The relationships of the mean/median values of basal microvilli length, density, and index with tumor PET-CT SUVmax values in pancreatic cancer patients. Spearman's correlations were used to estimate the correlation efficiency and statistical significance.

Table 2. Correlations of the basal microvilli parameters with clinicopathological variables in the pancreatic cancer patients.

	BMD1		BMD2		BML1		BML2		BMI1		BMI2	
	r	*p*	*r*	*p*	*r*	*p*	*r*	*p*	*r*	*p*	*r*	*p*
Gender, male versus female	0.1	0.313	0.083	0.404	0.154	0.12	0.175	0.077	0.125	0.209	0.107	0.282
Age, >60 versus <60	−0.034	0.735	−0.065	0.512	−0.029	0.733	−0.02	0.84	−0.022	0.089	−0.042	0.676
Tumor size	−0.061	0.54	−0.86	0.388	0.143	0.149	0.159	0.109	0.023	0.818	0.03	0.763
RLM (yes versus no)	**0.409**	**<0.001**	**0.416**	**<0.001**	**0.315**	**0.001**	**0.299**	**0.002**	**0.413**	**<0.001**	**0.409**	**<0.001**
TNM stage	**0.307**	**0.003**	**0.338**	**<0.001**	**0.412**	**<0.001**	**0.422**	**<0.001**	**0.377**	**<0.001**	**0.377**	**<0.001**
PNI (yes versus no)	0.11	0.268	0.068	0.492	−0.72	0.472	−0.69	0.488	0.029	0.772	0.011	0.915
MVI (yes versus no)	0.059	0.552	0.07	0.48	**0.253**	**0.01**	**0.233**	**0.018**	0.164	0.098	0.159	0.108
Tumor vascular thrombus (yes versus no)	**0.293**	**0.003**	**0.294**	**0.003**	**0.275**	**0.005**	**0.289**	**0.003**	**0.334**	**0.001**	**0.334**	**0.001**
Resection margin (R1 versus R0)	0.051	0.606	0.105	0.293	**0.218**	**0.027**	**0.233**	**0.018**	0.133	0.179	0.155	0.118
CA 19-9 (positive versus negative)	0.022	0.826	−0.04	0.97	−0.15	0.882	0.01	0.92	0.013	0.894	0.015	0.879
CEA (positive versus negative)	0.054	0.585	0.039	0.694	0.152	0.125	0.146	0.142	0.11	0.27	0.068	0.493
Ki67 index	0.19	0.056	**0.205**	**0.038**	0.186	0.061	**0.21**	**0.034**	**0.232**	**0.019**	**0.245**	**0.013**
Fasting blood glucose	0	0.999	0.013	0.898	0.096	0.338	0.096	0.338	0.048	0.629	0.065	0.52
Serum albumin levels	0.084	401	0.107	0.283	0.019	0.847	0.023	0.819	0.071	0.477	0.078	0.433

Spearman correlation, *r*, correlation efficiency; fasting blood glucose, before surgery; serum albumin levels, before surgery; tumor size, the largest diameters. BMD, basal microvilli density; BML, basal microvilli length; BMI, basal microvilli index; 1, mean; 2, median.
Bold font indicates statistically significant values.

values (29.6) and vice versa (supplementary material, Figure S2A). Correlation analysis indicated that basal microvilli parameters, such as length and density, correlated strongly with PET-SUVmax values [Figure 2B; length: $p < 0.001$, $r = 0.814$ (mean) and $r = 0.821$ (median); density: $p < 0.001$, $r = 0.718$ (mean) and $r = 0.737$ (median)]. The cellular surface of the basal microvilli was assessed by density and length; therefore, we used the 'basal microvilli index' value combined with the length and density parameters to estimate the total increase of endothelial surface area. The correlations of the basal microvilli index value with SUVmax on PET were more statistically significant than those between SUVmax and the length or density separately were (Figure 2B; mean: $p < 0.001$, $r = 0.866$; median: $p < 0.001$, $r = 0.869$). These strong correlations implied that the basal microvilli parameters could predict the glucose uptake of pancreatic cancer in terms of SUVmax on PET-CT, strongly supporting the notion that basal microvilli compensate for glucose transport from the hypomicrovasculature to the tumor milieu.

Clinically, our data showed that basal microvilli density and length and the basal microvilli index all strongly correlated with unfavorable pathological characteristics such as regional lymph node metastasis ($p < 0.002$), advanced TNM stage ($p < 0.003$), and tumor vascular thrombus ($p < 0.005$) (Table 2). Patients with longer and denser basal microvilli were more prone to having regional lymph node metastasis, advanced TNM stage, tumor vascular thrombus, and a high Ki67 index (Table 2). The basal microvilli length was also associated with margin-positive resection (R1) and major vascular invasion (Table 2). Univariate analysis showed that regional lymph node metastasis, advanced TNM stage, tumor thrombus, margin-positive resection, and major vascular invasion were significant risk factors in this cohort (Table 1). These results demonstrated that longer and denser basal microvilli in pancreatic cancer indicated higher metastatic or invasive and proliferative potential in neoplastic cells.

Longer and denser basal microvilli in pancreatic cancer are related to the dismal prognosis

Pieces of evidence suggest that pancreatic cancer patients with high PET-CT SUVmax values and lymph metastasis have a dismal prognosis [17,18,20]. In our previous work, we did not explore the clinical implications of basal microvilli. After obtaining the patients' follow-up data, we noticed that pancreatic cancer patients with a shorter relapse-free survival (RFS) have longer and denser basal microvilli on the tumor microvasculature, and vice versa (Figure 3A). Thus, basal microvilli may have the ability to predict relapse or death of pancreatic cancer patients. To test if basal microvilli parameters can predict relapse or death of pancreatic cancer patients, we carried out an ROC curve analysis. The results showed that all basal microvilli parameters, including density, length, and index, could predict the relapse or death of pancreatic cancer patients, and all the AUC (area under curves) values were higher than 0.649 (Figure 3B, C). We further analyzed the hazard ratios and survival functions of basal microvilli parameters by Cox regression and Kaplan–Meier methods. The analysis showed that patients with longer and denser basal microvilli had both significantly lower RFS and significantly lower OS days than patients with shorter and sparser basal microvilli [Figure 4A,B; supplementary material, Figure S3A, B; length: shorter versus longer, 419 versus 202 days (RFS); 998 versus 410 days (OS); density: thinner versus denser, 400 versus 233 days (RFS); 751 versus 467 days (OS)]. The hazard ratios of longer basal microvilli for RFS and OS rates were extremely high [supplementary material, Figure S3A,B; mean relapse, 2.304 (95% CI 1.548–3.693); mean survival, 3.990 (95% CI

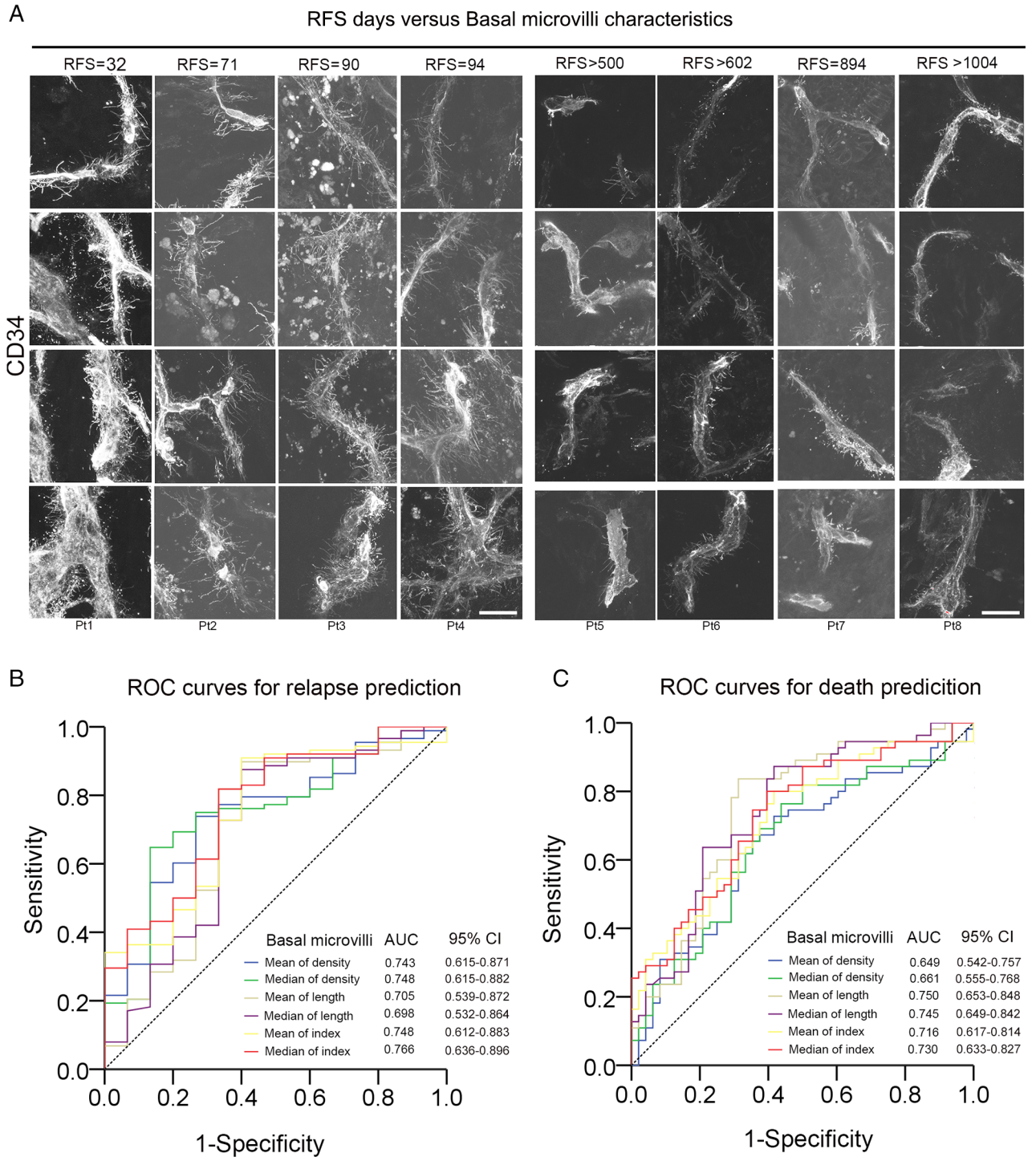

Figure 3. Basal microvilli parameters can predict the relapse and death of pancreatic cancer patients. (A) The basal microvilli patterns in eight patients with different RFS durations. A CD34 antibody was used to stain microvessels. All images were taken from an Z-stack and are shown as maximum intensity projection. Scale bar: 20 μm. (B, C) ROC curves of basal microvilli parameters for predicting (B) relapse and (C) death in pancreatic cancer patients.

2.053–6.598)]. The hazard ratio of longer basal microvilli for OS and RFS rates was higher than that of regional lymph node metastasis, histopathological grade, TNM stage, peripheral neuronal invasion, major vascular invasion, Ki67 index, serum CA 19-9 and CEA values, and was almost equal to that of the SUVmax value on PET (Table 1). These findings showed that basal microvilli parameters, such as length and density, indicate the prognosis of pancreatic cancer patients after surgery.

Longer and denser basal microvilli in pancreatic cancer are refractory to adjuvant therapy

In our cohort, 94 patients with basal microvilli received adjuvant therapy, including chemotherapy or

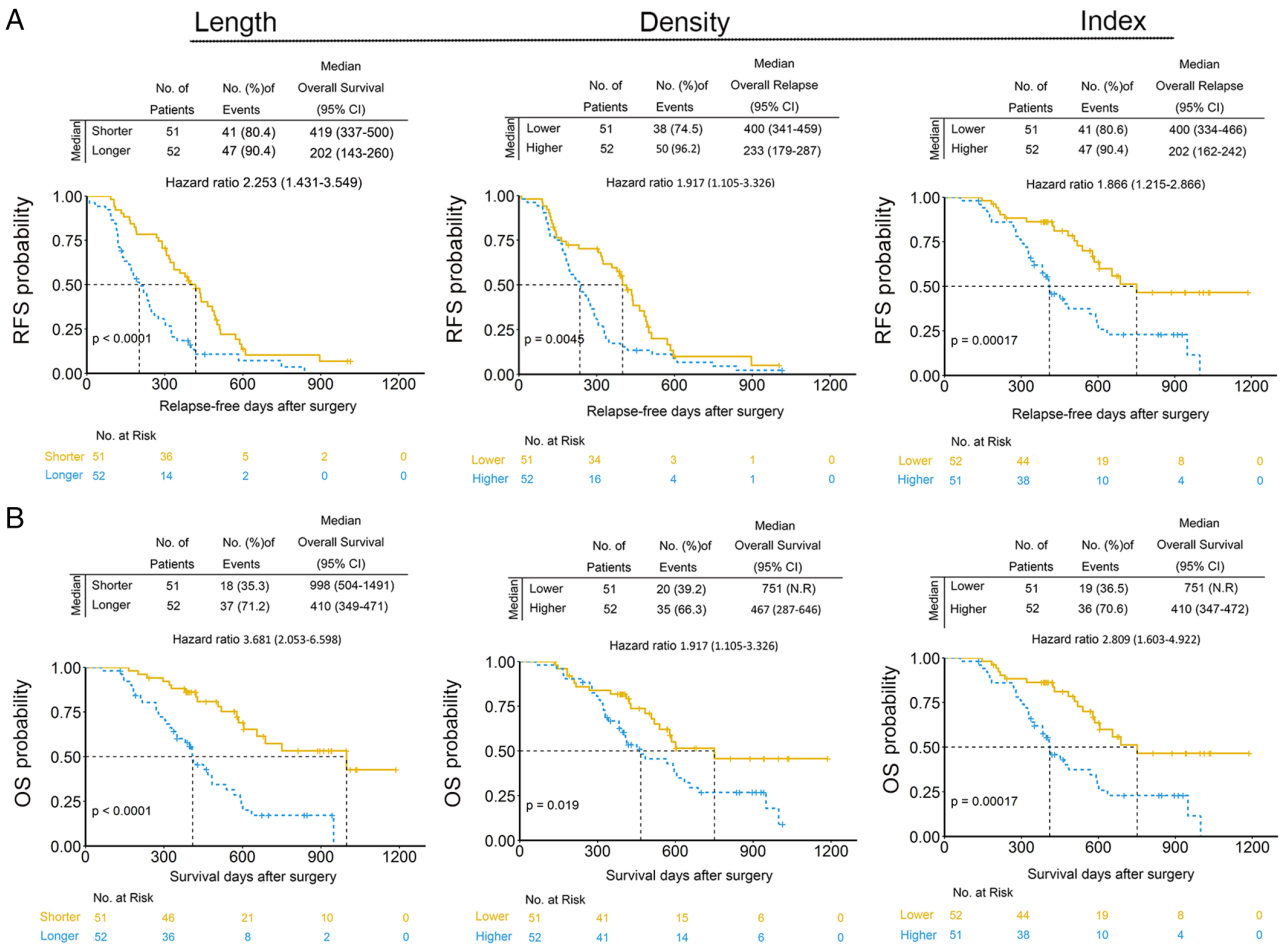

Figure 4. Pancreatic cancer patients with longer and denser basal microvilli have a dismal prognosis. (A, B) Kaplan–Meier curves for RFS and OS stratified by basal microvilli parameters in the cohort. Median values of basal microvilli length or density were used as a parameter (length: shorter, <11.17 μm; longer, ≥11.17 μm; density: lower, <6.04/100 μm^2; higher, ≥6.04/100 μm^2; index: lower, <2.14; higher, ≥2.14). Cox regression was used to assess the hazard ratios; the log-rank test was used to test the *P* values.

chemoradiotherapy, whereas nine patients did not receive any adjuvant treatment. In the adjuvant therapy subgroup, patients with longer and denser basal microvilli were more prone to have dismal outcomes than patients with shorter and sparser basal microvilli (Figure 5A,B and supplementary material, Figure S4A,B). In the adjuvant therapy subgroup, survival analysis also verified that patients with longer and denser basal microvilli had both significantly lower OS and significantly lower RFS rates than those with shorter and sparser basal microvilli [length: longer versus shorter, 217 versus 390 days (RFS) and 412 versus 998 days (OS); density: denser versus thinner, 237 versus 400 (RFS) and 467 versus 751 (OS)]. We observed that the median RFS and OS of pancreatic cancer patients with longer basal and denser microvilli were shorter than those of patients with shorter and thinner basal microvilli in the no-treatment subgroup [supplementary material, Figure S5; length: longer versus shorter, 116 versus 434 days (RFS) and 146 versus 585 days (OS); density: denser versus thinner, 112 versus 400 (RFS) and 112 versus 565 (OS)]. However, this analysis was carried out in a cohort of just nine patients (3 + 6) and the data are not significant. This finding suggested that basal microvilli parameters also indicate cancer cells' sensitivity to adjuvant therapies, including chemotherapy and chemoradiotherapy.

Discussion

Microvilli control the transport of metabolites and fluids in the polarized epithelial tissues, and their length and density decide the transporting capacity of fluid and metabolites in tissues [1,13]. By analyzing the basal microvilli parameters in 106 pancreatic cancer patients, we found that basal microvilli are common features of the microvasculature in pancreatic cancer. The basal microvilli parameters are equally effective in revealing glucose uptake capacity in pancreatic cancer tissues as PET-CT SUVmax values. They could predict the invasive, metastatic, and proliferative potential of neoplastic cells; prognosis; and therapeutic outcomes of adjuvant therapies.

Genetic and neoplastic cellular alterations are generally used to define the lethality of solid tumors [21]. To the best of our knowledge, basal microvilli are the first tumor-specific microvilli in the tumor microcirculation that indicate the cancer's lethality. Technically, basal

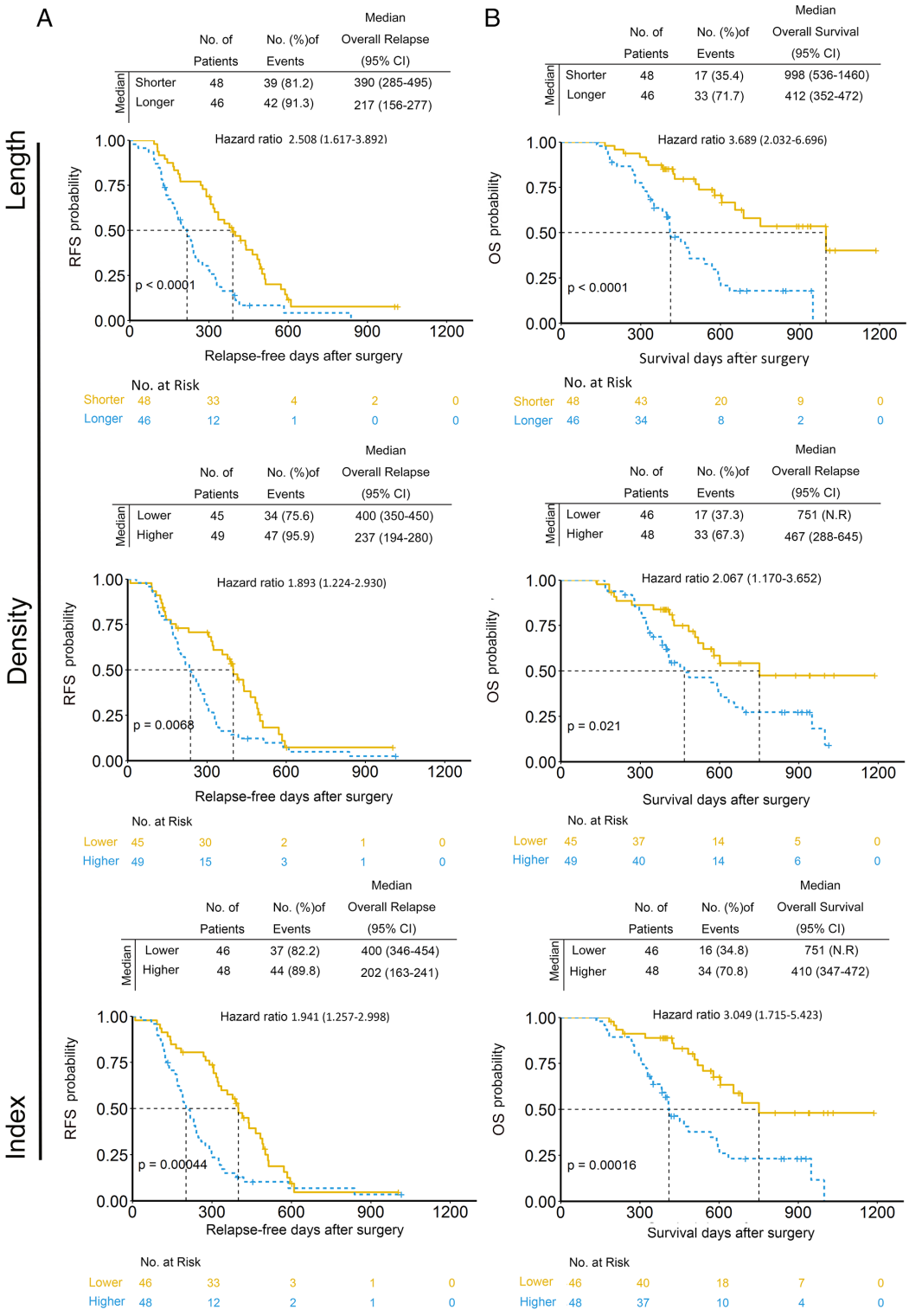

Figure 5. Pancreatic cancer patients with longer and denser basal microvilli are refractory to adjuvant therapy. (A, B) Kaplan–Meier curves for RFS and OS stratified by basal microvilli parameters in the postoperative adjuvant therapy subgroup. Median values of basal microvilli length or density were used as a parameter (length: shorter, <11.17 μm; longer, ≥11.17 μm; density: lower, <6.04/100 μm^2; higher, ≥6.04/100 μm^2; index: lower, <2.14; higher, ≥2.14). Cox regression was used to assess the hazard ratios; the log-rank test was used to test the *P* values.

microvilli are spatial cellular structures that can be visualized only with a 3D high-resolution scanning method. Thus, our findings imply the potential of 3D high-resolution imaging in visualizing tumor-specific structures, such as basal microvilli, and predicting the pathophysiological characteristics of neoplastic cells in clinical practice. Pathology is still the gold standard for clinical diagnosis and is critical for choosing the treatment regimen. The traditional pathological examination, which relies on the cellular morphology and the spatial arrangement of neoplastic cells, cannot provide precise information about tumor metabolism or the potential

metastatic or aggressive nature of neoplastic cells. However, not only are the basal microvilli cancer-specific but they could also provide information about metabolic preferences and the metastatic or invasive and drug-resistant potential of neoplastic cells *in vivo*.

More than 90% of all pancreatic cancers harbor *KRAS* mutations [22]. *RAS*-mutated tumors heavily depend on the Warburg effect – glycolysis to obtain energy for ATP generation [23,24]. The basal microvilli represent systematic changes in the pancreatic microcirculation and are abundant in tumor tissues with elevated glucose uptake. Microvilli of the syncytiotrophoblast in the placenta facilitate the bidirectional exchanges between mother and fetus [13]. In the intestine, microvilli increase the apical surface area by 9.2–15.7 times [25]. In the pancreatic microvasculature, the presence of basal microvilli increases the basal surface area by nearly 0.69–6.07 times. Thus, the microvasculature with basal microvilli might create a 'super' microvessel network that is a highly efficient and sustainable shuttle system for transporting glucose and metabolites but not oxygen, perfectly compensating for the hypomicrovascularity in pancreatic cancers. Basal microvilli selectively transport necessities such as nutrients to, or waste from, tumors but not chemotherapeutic drugs. The selective trafficking of basal microvilli might explain our findings that pancreatic cancers with longer and denser basal microvilli are refractory to gemcitabine-based adjuvant therapy and support the notion that basal microvilli might not efficiently deliver gemcitabine to the tumor milieu. Basal microvilli contain caveolae, which are clathrin-independent trafficking vesicles [11,26]. Albumin is reliant on caveolae-mediated endocytosis to be transported or absorbed in pancreatic cancer [27]. Thus, nab-paclitaxel (Abraxane) in pancreatic cancers might cling onto basal microvilli to be transported to cells within the tumor milieu [28].

Our findings also raise several questions concerning the innate characteristics of basal microvilli. Contrary to apical microvilli in other epithelia, basal microvilli appear on the basal surface of endothelial cells in pancreatic cancers. How can these microvessels with basal microvilli traffic nutrients to the tumor milieu? What are the cues for the tumor milieu to induce endothelial cells to form basal microvilli? Currently, high-throughput screening technologies can easily provide candidate cues for basal microvilli. However, a suitable model of basal microvilli *in vitro* and *in vivo* is necessary to decode the mechanisms behind the formation of these basal microvilli. Troubling us is the fact that the basal microvilli of human pancreatic cancers decline significantly and diminish quickly when cultured *in vitro* [12]. This finding suggests that the growth and maintenance of basal microvilli might rely on blood flow. We also discovered basal microvilli in *KRAS*-mutated autochthonous pancreatic cancers of mice but not in orthotopic pancreatic cancers of mice [11,12,29]. However, the sizes of these tumors in mice are far smaller than those in human cancers. Accordingly, whether autochthonous pancreatic cancer mice are suitable for exploring the regulatory molecules of basal microvilli is questionable.

Collectively, our data showed that the abundance of basal microvilli defines the glucose metabolic capacity and lethal phenotype of pancreatic cancers, indicating that basal microvilli are an anatomical tunnel to deliver drugs or starve neoplastic cells. These results also highlight the emerging role of basal microvilli and suggest an expanding utility in future pathology or clinical practices in pancreatic cancer.

Acknowledgements

This study was supported by grants from the National Natural Science Foundation (81702304) and SinoGerman Precision Medicine in Pancreatic Cancer (GZ1456).

Author contributions statement

HS and WHL conceptualized the design. HS, XH, WHL, LJ and DLF set up this project. XH and JG collected fresh samples and performed the follow-up for the patients. LXM coordinated the tissue collection. LXM, WHL, XH, JL and DLF provided support for the projects, including from the National Natural Science Foundation (81702304) and SinoGerman Precision Medicine in Pancreatic Cancer (GZ1456). LXM and HS performed all staining, scanning, and measuring of the basal microvilli. HS and XH analyzed the data and wrote the paper.

References

1. Lange K. Fundamental role of microvilli in the main functions of differentiated cells: outline of an universal regulating and signaling system at the cell periphery. *J Cell Physiol* 2011; **226:** 896–927.
2. Crawley SW, Mooseker MS, Tyska MJ. Shaping the intestinal brush border. *J Cell Biol* 2014; **207:** 441–451.
3. Halberg KA, Rainey SM, Veland IR, *et al*. The cell adhesion molecule Fasciclin2 regulates brush border length and organization in *Drosophila* renal tubules. *Nat Commun* 2016; **7:** 11266.
4. Coudrier E, Kerjaschki D, Louvard D. Cytoskeleton organization and submembranous interactions in intestinal and renal brush borders. *Kidney Int* 1988; **34:** 309–320.
5. Gresham GK, Wells GA, Gill S, *et al*. Chemotherapy regimens for advanced pancreatic cancer: a systematic review and network meta-analysis. *BMC Cancer* 2014; **14:** 471.
6. O'Reilly EM, Oh DY, Dhani N, *et al*. Durvalumab with or without tremelimumab for patients with metastatic pancreatic ductal adenocarcinoma: a phase 2 randomized clinical trial. *JAMA Oncol* 2019; **5:** 1431–1438.
7. Chin V, Nagrial A, Sjoquist K, *et al*. Chemotherapy and radiotherapy for advanced pancreatic cancer. *Cochrane Database Syst Rev* 2018; **3:** CD011044.
8. Davidson SM, Jonas O, Keibler MA, *et al*. Direct evidence for cancer-cell-autonomous extracellular protein catabolism in pancreatic tumors. *Nat Med* 2017; **23:** 235–241.
9. Neesse A, Algul H, Tuveson DA, *et al*. Stromal biology and therapy in pancreatic cancer: a changing paradigm. *Gut* 2015; **64:** 1476–1484.
10. Yan L, Raj P, Yao W, *et al*. Glucose metabolism in pancreatic cancer. *Cancers (Basel)* 2019; **11:** 1460.

11. Saiyin H, Ardito-Abraham CM, Wu Y, *et al*. Identification of novel vascular projections with cellular trafficking abilities on the microvasculature of pancreatic ductal adenocarcinoma. *J Pathol* 2015; **236:** 142–154.
12. Ma L, Han X, Gu J, *et al*. The physiological characteristics of the basal microvilli microvessels in pancreatic cancers. *Cancer Med* 2020; **9:** 5535–5545.
13. Friederich E, Louvard D. In *Encyclopedic Reference of Genomics and Proteomics in Molecular Medicine*, Ganten D, Ruckpaul K (eds). Springer: Berlin, 2006; 1116–1121.
14. Iancu TC, Mahajnah M, Manov I, *et al*. Microvillous inclusion disease: ultrastructural variability. *Ultrastruct Pathol* 2007; **31:** 173–188.
15. Ruemmele FM, Schmitz J, Goulet O. Microvillous inclusion disease (microvillous atrophy). *Orphanet J Rare Dis* 2006; **1:** 22.
16. Yamamoto T, Sugiura T, Mizuno T, *et al*. Preoperative FDG-PET predicts early recurrence and a poor prognosis after resection of pancreatic adenocarcinoma. *Ann Surg Oncol* 2015; **22:** 677–684.
17. Okazaki E, Seura H, Hasegawa Y, *et al*. Prognostic value of the volumetric parameters of dual-time-point ^{18}F-FDG PET/CT in non-small cell lung cancer treated with definitive radiation therapy. *Am J Roentgenol* 2019; **213:** 1366–1373.
18. Schellenberg D, Quon A, Minn AY, *et al*. ^{18}Fluorodeoxyglucose PET is prognostic of progression-free and overall survival in locally advanced pancreas cancer treated with stereotactic radiotherapy. *Int J Radiat Oncol Biol Phys* 2010; **77:** 1420–1425.
19. Asagi A, Ohta K, Nasu J, *et al*. Utility of contrast-enhanced FDG-PET/CT in the clinical management of pancreatic cancer: impact on diagnosis, staging, evaluation of treatment response, and detection of recurrence. *Pancreas* 2013; **42:** 11–19.
20. Sheikhbahaei S, Wray R, Young B, *et al*. ^{18}F-FDG-PET/CT therapy assessment of locally advanced pancreatic adenocarcinoma: impact on management and utilization of quantitative parameters for patient survival prediction. *Nucl Med Commun* 2016; **37:** 231–238.
21. Loberg RD, Bradley DA, Tomlins SA, *et al*. The lethal phenotype of cancer: the molecular basis of death due to malignancy. *CA Cancer J Clin* 2007; **57:** 225–241.
22. Ryan DP, Hong TS, Bardeesy N. Pancreatic adenocarcinoma. *N Engl J Med* 2014; **371:** 1039–1049.
23. Ying H, Kimmelman AC, Lyssiotis CA, *et al*. Oncogenic Kras maintains pancreatic tumors through regulation of anabolic glucose metabolism. *Cell* 2012; **149:** 656–670.
24. Bryant KL, Mancias JD, Kimmelman AC, *et al*. *KRAS*: feeding pancreatic cancer proliferation. *Trends Biochem Sci* 2014; **39:** 91–100.
25. Helander HF, Fandriks L. Surface area of the digestive tract – revisited. *Scand J Gastroenterol* 2014; **49:** 681–689.
26. Pepperkok R, Scheel J, Horstmann H, *et al*. β-COP is essential for biosynthetic membrane-transport from the endoplasmic reticulum to the Golgi complex *in vivo*. *Cell* 1993; **74:** 71–82.
27. Chatterjee M, Ben-Josef E, Robb R, *et al*. Caveolae-mediated endocytosis is critical for albumin cellular uptake and response to albumin-bound chemotherapy. *Cancer Res* 2017; **77:** 5925–5937.
28. Von Hoff DD, Ramanathan RK, Borad MJ, *et al*. Gemcitabine plus nab-paclitaxel is an active regimen in patients with advanced pancreatic cancer: a phase I/II trial. *J Clin Oncol* 2011; **29:** 4548–4554.
29. Ma L, Saiyin H. *LSL-Kras^{G12D}; LSL-Trp53$^{R172H/+}$; Ink4$^{flox/+}$; Ptf1/p48-Cre* mice are an applicable model for locally invasive and metastatic pancreatic cancer. *PLoS One* 2017; **12:** e0176844.

SUPPLEMENTARY MATERIAL ONLINE

Figure S1. Basal microvilli patterns

Figure S2. Basal microvilli patterns in pancreatic cancer with an SUVmax of 29.6 on PET-CT and another case with an SUVmax of 4.6 on PET-CT

Figure S3. Longer and denser basal microvilli in pancreatic cancer are related to dismal prognosis (related to Figure 3)

Figure S4. Longer and denser basal microvilli in pancreatic cancer are refractory to adjuvant therapy (related to Figure 4)

Figure S5. Longer and denser basal microvilli in pancreatic cancer are related to dismal prognosis in the no-treatment group (related to Figure 4)

Table S1. Antibodies, equipment, and software list

Table S2. Values of the basal microvilli density, length, and index in 106 pancreatic cancer patients